Protein Science (1999), *8*:1232–1240. Cambridge University Press. Printed in the USA.

The molecular structure of an unusual cytochrome c_2 determined at 2.0 Å; the cytochrome c_H from *Methylobacterium extorquens*

JON READ, RAJ GILL, SIMON L. DALES, JON B. COOPER, STEVE P. WOOD, AND CHRIS ANTHONY

Division of Biochemistry and Molecular Biology, School of Biological Sciences, University of Southampton, Southampton SO16 7PX, United Kingdom

(RECEIVED December 15, 1998; ACCEPTED February 25, 1999)

Abstract

Cytochrome c_H is the electron donor to the oxidase in methylotrophic bacteria. Its amino acid sequence suggests that it is a typical Class I cytochrome *c*, but some features of the sequence indicated that its structure might be of special interest. The structure of oxidized cytochrome c_H has been solved to 2.0 Å resolution by X-ray diffraction. It has the classical tertiary structure of the Class 1 cytochromes *c* but bears a closer gross resemblance to mitochondrial cytochrome *c* than to the bacterial cytochrome c_2. The left-hand side of the haem cleft is unique; in particular, it is highly hydrophobic, the usual water is absent, and the "conserved" Tyr67 is replaced by tryptophan. A number of features of the structure demonstrate that the usual hydrogen bonding network involving water in the haem channel is not essential and that other mechanisms may exist for modulation of redox potentials in this cytochrome.

Keywords: cytochrome c_H; cytochrome c_2; *Methylobacterium*; tryptophan; X-ray structure

During growth of methylotrophic bacteria on methane or methanol, energy is obtained from the oxidation of methanol catalyzed by a soluble quinoprotein methanol dehydrogenase (MDH). This occurs in the periplasm and initiates a short electron transport chain, which involves cytochrome c_L (the electron acceptor for the dehydrogenase) and cytochrome c_H (the donor to the oxidase) (Anthony, 1992):

$$\text{MDH} \rightarrow \text{Cytochrome } c_L \rightarrow \text{Cytochrome } c_H \rightarrow \text{Oxidase.}$$

To study the processes of intraprotein and interprotein electron transport, we are investigating the structures of these soluble proteins in *Methylobacterium extorquens*. The structure of the quinoprotein methanol dehydrogenase has been published previously (Ghosh et al., 1995; Anthony & Ghosh, 1998), and this paper describes the structure of the donor to the oxidase, cytochrome c_H. Its amino acid sequence (Anthony, 1992) is typical of mitochondrial cytochromes *c* and bacterial cytochromes c_2 that donate electrons to oxidases or photosynthetic reaction centers. These Class I cytochromes *c* are characteristically low spin with the single haem group attached covalently to the protein through thioether linkages between haem vinyl groups and two cysteine residues located near the N-terminus, the 5th ligand to the haem iron being histidine and the 6th ligand being methionine (Moore & Pettigrew, 1990). They share a common polypeptide fold that leads to the burial of the haem propionate substituents within the protein interior. Of the 96 sequences of cytochrome *c* listed by Moore and Pettigrew, 26% of residues are invariant and most of these are also conserved in the bacterial cytochromes c_2. Furthermore, the main features of these cytochromes are superimposable in the X-ray structures.

Within the cytochromes *c* and cytochrome c_2, the most significant differences occur within the "left-hand" side of the haem cleft in which Met80 is bonded to the haem iron. It is the properties of the residues in this region that are thought to determine differences in redox potential, and small changes in structure in this region between the oxidized and reduced conformations are proposed to have important implications with respect to mechanisms of electron transfer (Brayer & Murphy, 1996). Of particular importance are Tyr67, which is hydrogen bonded to the sulfur atom of Met80 in the ferrocytochrome; Thr78, which is hydrogen bonded to the outer haem propionate; and Arg38, which is hydrogen bonded to the inner propionate. A water molecule in this region is also conserved in most structures in which it is hydrogen bonded to Tyr67 and Thr78.

Although the primary sequence of cytochrome c_H is very similar to that of other cytochromes *c*, a few unusual features suggest that it might be of special interest with respect to the currently accepted

Reprint requests to: Professor Chris Anthony, Division of Biochemistry and Molecular Biology, School of Biological Sciences, University of Southampton, Southampton SO16 7PX, United Kingdom; e-mail: C.Anthony@soton.ac.uk.

conclusions concerning the role of the conserved residues in the vicinity of the haem. The X-ray structure of cytochrome c_H reported here confirms that this is indeed the case. For example, the absence of the "conserved" water, the substitution of Tyr67 by tryptophan, and the substitution of Arg38 by alanine prevent the establishment of the typical hydrogen bonded network in the haem channel that is considered to be important in modulating redox potentials and electron transfer events in other Class I *c*-type cytochromes.

Results and discussion

The primary sequence of cytochrome c_H

The primary sequence of cytochrome c_H (100 residues) has been previously determined by Ambler and Athalye (cited in Anthony, 1992). During model building of the X-ray structure, it proved possible to fit the entire sequence within the electron density except for the loop containing residues 38–42. To resolve this anomaly, a peptide containing this part of the sequence was produced by digestion with trypsin, and its sequence shown by Edman degradation to be 37-AGEGADGYAFSDA-49, thus reordering residues 41 to 43 from GAD to ADG. This sequence correlated well with the electron density and was used subsequently in model building. The sequence of cytochrome c_H is presented in Figure 1 aligned with sequences of mitochondrial cytochromes *c* from tuna, horse, and yeast, and some cytochromes c_2 whose X-ray structures have been determined. The alignment shows that between 43 and 45% of residues of cytochrome c_H are identical to those in cytochromes *c* and c_2. Although its sequence shows that cytochrome c_H is clearly a typical cytochrome c_2, for convenience in this paper we will continue to refer to it as cytochrome c_H.

The overall structure of cytochrome c_H

The structure of cytochrome c_H was determined by molecular replacement and refined to an *R*-factor of 16.5% with a corresponding R_{free} of 22.2% (see Materials and methods). The polypeptide chain backbones had continuous electron density for all three molecules in the triclinic unit cell. Side chains were partially disordered for all the three molecules in residues Lys9, Glu21, Lys22, Lys30, Lys36, Glu39, Lys52, and Lys63. The average main-chain thermal parameters (*B*-factors) for all three molecules in the unit cell are shown in Figure 2. The main-chain torsion angles for all three molecules in the unit cell were used for construction of the Ramachandran plot, which showed no residues in disallowed regions, and 88% of residues within the most favored regions as defined in the PROCHECK program used for this analysis (Laskowski et al., 1993).

Cytochrome c_H has the classical tertiary structure of the Class 1 cytochromes *c* and c_2, as shown in Figure 3. This comprises five helices (A to E) and their interconnecting loops, which together enclose the haem prosthetic group whose edge breaches the "front" face of the molecule where close approach with redox couple partners is thought to occur during electron transfer. It is notable that cytochrome c_H bears a closer gross resemblance to cytochrome *c* than to the bacterial cytochrome c_2; the main-chain atoms for cytochrome c_H and tuna cytochrome *c* superimpose with a root-mean-square deviation (RMSD) of 0.77 Å for 90 residues; for cytochrome c_H and cytochrome c_2 of *Rhodospirillum rubrum*, the RMSD is 0.85 Å for 87 residues.

```
                  -5    1        10        20        30        40          50
Yeast              TEFKAGSAKKGATLFKTRCLQCHTVEKGGPHKVGPNLHGIFGRHSGQAE-GYSTYTDA
Horse                   GDVEKGKKIFVQKCAQCHTVEKGGKHKTGPNLHGLFGRKTGQAP-GF-TYTDA
Tuna                    GDVAKGKKTFVQKCAQCHTVENGGKHKVGPNLWGLFGRKTGQAE-GY-SYTDA
                        1        10        20        30        40
Methylobacterium        EGDAAAGEKAFA-PCKACHNFEKNG---VGPTLKGVVGAKAGEGADGYA-FSDA
Rhodopila          GSAPPGDPVEGKHLFHTICILCHTDIKG-RNKVGPSLYGVVGRHSGIEP-GYN-YSEA
                        1        10        20        30        40          50
Rhodospirillum          EGDAAAGEKVSK-KCLACHTFDQGGANKVGPNLFGVFENTAAHKD-NYA-YSES

                                 60        70                80        90          112
Yeast                   NIK---KNVLWDENNMSEYLTNP-KYIPG--------TKMAFAGLKKEKDRNDITYLKKACE
Horse                   NKN---KGITWKEETLMEYLENPKKYIPG--------TKMIFAGIKKKTEREDLIAYLKKATNE
Tuna                    NKS---KGIVWNENTLMEYLENPKKYIPG--------TKMIFAGIKKKGERQDLVAYLKSATS
                        50          60        70                80        90          100
Methylobacterium        LKK---SGLTWDQADLKQWLADPKKKVPG--------TKMVFPGISDPKKVDDIIAYLKTKS
Rhodopila               NIK---SGIVWTPDVLFKYIEHPQKIVPG--------TKMGYPGQPDPQKRADIIAYLETLK
                                60        70        80        90        100         112
Rhodospirillum          YTEMKAKGLTWTEANLAAYVKDPKAFVLEKSGDPKAKSKMTFKLTKDDE-IENVIAYLKTLK
```

Fig. 1. The sequence of cytochrome c_H of *M. extorquens*. This is aligned with sequences of cytochromes whose structures have been determined; these include the mitochondrial cytochrome *c* from horse heart (Bushnell et al., 1990; Qi et al., 1994; Banci et al., 1997b), tuna (Tanako & Dickerson, 1981a, 1981b), and yeast (*Saccharomyces cerevisiae* iso-I-cytochrome *c*) (Louie & Brayer, 1990; Baistrocchi et al., 1996; Benning et al., 1996; Banci et al., 1997a); and the cytochromes c_2 from *Rhodopila globiformis* (Benning et al., 1996) and *R. rubrum* (Salemme et al., 1973). Sequences are taken from Moore and Pettigrew (1990). The numbers refer to the tuna mitochondrial cytochrome *c* (upper), *M. extorquens* (middle), and *R. rubrum* (lower). The residues marked in bold are those that are different in cytochrome c_H and which have a major influence on the properties of the left hand side of the haem cleft. The underlined sequence is the loop that is relatively more rigid in cytochrome c_H.

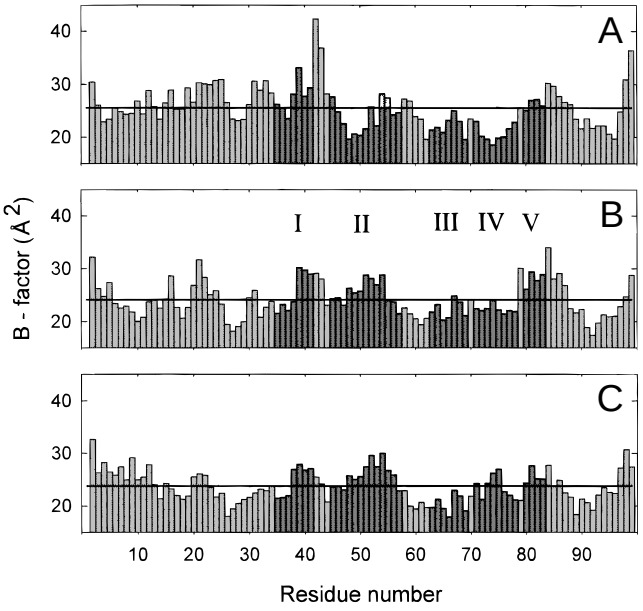

Fig. 2. The *B*-factors for the main-chain atoms of cytochrome c_H. The mean *B*-factors are represented in each case by a horizontal line. Regions of the molecule that are referred to in the text are marked as dark bars.

The α-helix A (residues 4 to 15) is distorted by Pro13 (see Fig. 3) that replaces an otherwise conserved lysine (tuna, Lys13) on the surface, and this change allows solvent access to atom CBB on the haem. The sequence of residues 15 through 39 is composed of a series of turns. The loop (18 to 29) immediately after the haem binding sequence (CKACH) is three residues shorter than in cytochromes *c* and c_2 and encloses a buried water molecule in all three cytochromes (Wat4 in cytochrome c_H). The base loop (36 to 39) has an insertion of one residue and therefore adopts a slightly different conformation from that in cytochromes *c* and c_2; furthermore, the otherwise conserved arginine (tuna Arg38) is replaced by Ala35 in cytochrome c_H. Helix B (41 to 43) is short (about one turn in length) and is followed by a portion of "random coil" similar in conformation to cytochrome *c*. Helix C (59 to 67) consists of two full turns as seen in cytochrome c_2 and contains a unique tryptophan substitution (Trp65) toward its C-terminus, replacing Tyr67 in tuna cytochrome *c*. Helix D (69 to 72) is only four residues long as in cytochrome *c*, and the subsequent extended chain (73 to 86) also follows a similar path. The last helix (E) (residues 86 to 97) is intermediate in length (about three turns) between the E helices of cytochrome c_2 (2.5 turns) and cytochrome *c* (four turns). The terminal helices (A and E) are held together by way of a van der Waals interaction between aromatic side chains (Phe10 and Tyr95) on the two helices exactly as seen in tuna cytochrome *c*.

In cytochromes *c* and c_2, the residues immediately surrounding the haem edge facing the solvent are mainly hydrophobic and the five closest of these are conserved as hydrophobic residues in cytochrome c_H (Moore & Pettigrew, 1990; Brayer & Murphy, 1996); these are Ala12 (tuna, Val11), Val25 (Val28), Tyr44 (Tyr46), Val79 (Ile81), Phe80 (Phe82), and Pro81 (Ala83). Ala15 is replaced with Lys15. Only two out of the five acidic residues of tuna are acidic in cytochrome c_H; one of these is the highly conserved Asp91 (tuna, Asp93). Of the 12 lysine residues present on the front face of tuna cytochrome *c*, only four are present in cytochrome c_H (Lys9, Lys70, Lys71, and Lys77); these include the three that are conserved in all cytochromes *c* and c_2 and which are thought to be important in interactions with redox partners (tuna, Lys72, Lys73, and Lys79).

Because the overall structure of cytochrome c_H is generally similar to other cytochromes *c* and c_2, we can conclude that interaction with its redox partners is by way of bonding between hydrophobic residues around the haem edge, following an initial ionic interaction involving the conserved lysines, as shown previously by chemical modification and cross linking studies (Anthony, 1992; Cox et al., 1992).

The flexibility of the cytochrome c_H backbone

Figure 2 shows the mean *B*-values for the main-chain atoms of oxidized cytochrome c_H for each of the three molecules in the unit cell; the regions showing the greatest flexibility (higher *B*-values) are, as expected, the loop regions. The loop leading to the methionine ligand (Lys71–Met78; indicated by IV in Fig. 2) is relatively immobile as seen in other cytochromes *c*. In these cytochromes there is a salt bridge between the "invariant arginine" (tuna, Arg38) and the inner haem propionate, the loop carrying this arginine being relatively rigid and showing little change on reduction. By contrast, in cytochrome c_H, Arg38 is replaced by Ala35 and therefore, as expected, the loop between Ala35 and Ala41 (indicated by I in Fig. 2) is relatively mobile. In cytochromes *c* three other loops are relatively mobile (yeast numbering: 47–59, 65–72, 81–85). In cytochrome c_H two of these are also mobile; these are region II (Ala45–Trp57), and region V (Lys79–Ile83). The third of these loops (III; Lys63–Pro70), however, is relatively rigid; this is the loop that contains the conserved tyrosine in cytochromes *c* and c_2 (tuna, Tyr67), which is uniquely replaced by tryptophan (Trp65), leading to a generally more rigid structure in this region in cytochrome c_H.

The hydrophobic environment of the haem in cytochrome c_H

In cytochrome c_H many of the interactions with the haem are very similar to those in all other cytochromes *c* and c_2. The haem is covalently bonded to the protein by thioether linkages from Cys14 and Cys17, and the haem iron is ligated to His18 and Met78; the bond length between S of Met78 and the haem iron atom is 2.27 Å, that between $N^{\epsilon 2}$ of His18 and the haem iron is 1.91 Å, and the angle formed between these bonds is 174.4°. Except for some of the interactions with the haem propionates, all other interactions are predominantly hydrophobic in character including those involving Trp57 (tuna, Trp59), Phe80 (Phe82), Pro69 (Pro71) on the left of the haem (with respect to the conventional view as seen in Fig. 3), and Leu66 (Leu68) behind the methionine. However, the following replacements near the haem of cytochrome c_H are more hydrophobic than in cytochrome *c*: Trp65 (tuna, Tyr67), Ala35 (tuna, Arg38), Phe46 (Tyr48), and Leu50 (Asn52).

In cytochrome c_H, as in most cytochromes *c* and c_2 , the outer haem propionate (HP6, on haem ring D) has no direct interaction with solvent; it forms hydrogen bonds with side chains of buried threonine or serine and the main-chain nitrogen atom of a lysine residue (Table 1; Fig. 4). The inner haem propionate (HP7, on ring A) is exceptional in cytochrome c_H in not being shielded completely from solvent (Fig. 5). Although the bonding of one oxygen atom (O2A) is similar to that in cytochrome *c* (Table 1, Fig. 6), the

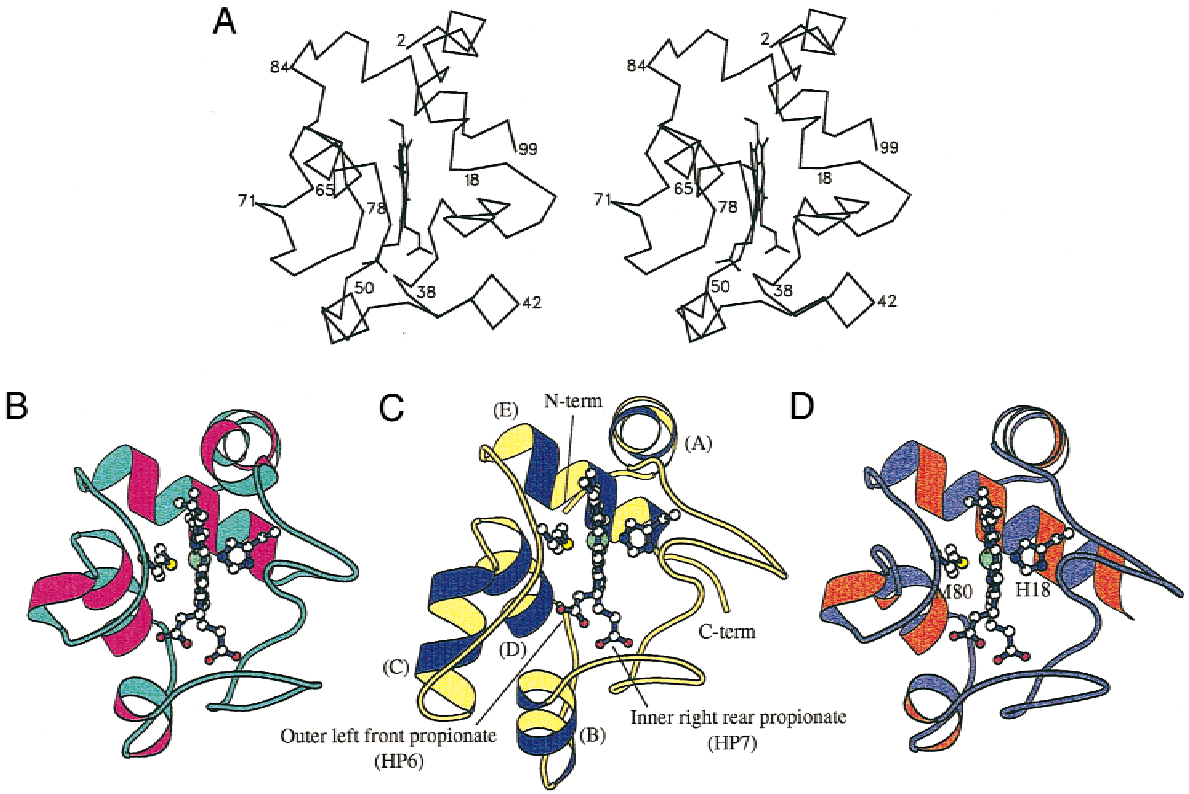

Fig. 3. The overall folds of cytochrome c_H, cytochrome *c*, and cytochrome c_2. **A:** Stereo view of the C_α trace of cytochrome c_H. **B:** Cytochrome c_H. **C:** Cytochrome c_2 from *R. rubrum*. **D:** Tuna cytochrome *c*. The colored structures are presented in the same view as that presented in the stereo view of cytochrome c_H.

other oxygen atom (OA1) is bonded completely differently. This atom is usually protected from bulk solvent by hydrogen bonding to one of the conserved waters (tuna, Wat26) and to the conserved Tyr48 (tuna) and Arg38 (tuna) (Fig. 6). In cytochrome c_H, the propionate oxygen (O1A) is also hydrogen bonded to water (Wat1; tuna, Wat26), but Tyr48 and Arg38 (tuna) are replaced by the nonbonding Phe46 and Ala35. The space usually taken by the arginine side chain is occupied by a second water (Wat2), which is hydrogen bonded to the propionate (O1A) and to water in contact with bulk solvent (Table 1; Figs. 6, 7). It is possible that dissociation of this exceptionally exposed "inner" propionate contributes to the unusual pH dependence of redox potential previously reported for this cytochrome (O'Keeffe & Anthony, 1980).

A unique feature of the haem cleft of cytochrome c_H

Of the three buried conserved water molecules present in cytochromes *c* and c_2, only two are present in cytochrome c_H. One of these is Wat4 (tuna, Wat2), adjacent to the histidine ligand; the second Wat1 (tuna, Wat26) is located toward the outside of the cleft and is bonded to main-chain oxygen and nitrogen atoms and to the inner propionate (HP7) (Table 1; Fig. 6). At the entrance of the haem cleft in cytochrome c_H, there is an additional water (Wat2) occupying the position of the side chain of Arg38 (in tuna), which is replaced in cytochrome c_H by Ala35 (Fig. 6). This water is in direct contact with bulk solvent (Fig. 5) and is also linked to the inner haem propionate (HP7).

The majority of cytochromes *c* and c_2 contain a third buried water molecule (Wat3 in tuna; Wat166 in yeast) in the left-hand side of the haem cleft where it is hydrogen bonded to a conserved tyrosine (tuna, Tyr67) (Scott & Mauk, 1996; Surridge, 1994). Remarkably, in cytochrome c_H this tyrosine is replaced by tryptophan (Trp65) whose bulk precludes the possibility of a buried water molecule in this location (Table 1; Fig. 7).

It should be noted that cytochrome c_2 of *R. rubrum* is also unusual in lacking the "conserved" buried water but this is replaced by a second tyrosine (Tyr52) whose hydroxyl oxygen atom replaces the water oxygen and forms a hydrogen bonding network with Tyr70 (tuna, Tyr67) and Ser89 (tuna, Thr78) in the ferricytochrome (Table 1; Fig. 4) (Salemme et al., 1973).

The redox potential of cytochrome c_H

Factors affecting redox potentials of cytochromes include local dielectric effects arising from the amount of solvent exposed haem, the presence of more or less hydrophobic residues near the haem, the orientation of the haem ligands relative to the haem plane, the extent of hydrogen bonding to these ligands and the haem propionates, and solvent structure in the haem binding pocket (Moore & Pettigrew, 1990). For example, a more hydrophobic environment in the haem pocket will favor the reduced form and raise the redox potential Kassner (1972). The redox potential of cytochrome c_H (294 mV) is 34 mV higher than that of mitochondrial cytochrome (O'Keeffe & Anthony, 1980), which is consistent with the lack of

Table 1. *The coordination of water and propionates in cytochrome c of tuna, cytochrome c_2 of R. rubrum and cytochrome c_H*[a]

	Coordinating species		
	Cytochrome *c* Tuna	Cytochrome c_2 *R. rubrum*	Cytochrome c_H *M. extorquens*
Water; Wat26, Wat1	O2A of HP7 (inner haem) 2.6 Å	Water replaced by His42	O1A of HP7 (inner haem) 2.8 Å
	Gln42 N 2.9 Å		Glu39 N 2.8 Å
	Lys39 O 2.8 Å		Lys36 O 3.1 Å
			Gly40 N 2.7 Å
Water; Wat3	Tyr67 OH 2.9 Å	Water replaced by OH of Tyr52	Trp57 excludes water
	Thr78 OG1 2.9 Å		
	Asn52[b] ND1 3.0 Å		
Tyr52 of *R. rubrum* (This replaces Wat3.)		Tyr70 OH 2.7 Å Ser89 OG 2.4 Å	
Inner haem propionate (HP7)			
O1A	Wat26 O 2.6 Å		Wat1 O 2.8 Å
	Tyr48 OH 2.7 Å	Tyr48 OH 2.7 Å	Phe46 cannot bond
	Arg38 NH1 2.8 Å	His42 N 2.9 Å	Ala35 cannot bond
		His42 ND1 2.2	Wat2 O 2.9 Å
O2A	Trp59 NE1 3.0 Å	Trp62 NE1 3.0 Å	Trp57 NE1 2.9 Å
	Gly41 N 3.3 Å	Ala41 N 2.9 Å	Gly38 N 2.8 Å
	Asn52[b] OD 3.2 Å	Tyr42 not bonded	Leu50 cannot bond
Outer haem propionate (HP-6)			
O1D	Thr49 N 3.0 Å	Ser49 N 2.9 Å	Ser47 not bonded
O2D	Thr49 OG1 2.7 Å	Thr49 OG1 2.6 Å	Ser47 OG1 2.8 Å
			Ser47 N 2.7 Å
	Thr78 OG1 2.7 Å	Ser89 not bonded	Thr76 OG 2.6 Å
	Lys79 N 3.1 Å	Lys90 N 2.6 Å	Lys77 N 2.9 Å

[a]In all the bonds identified in the table, the residues involved are equivalent in the sequence (see Fig. 1), except that Arg38 in cytochrome *c* is replaced by His42 in *R. rubrum* cytochrome c_2.
[b]Asn52 is bonded to Wat3 and propionate only in the reduced cytochrome.

water molecules and the remarkable number of hydrophobic substitutions in this region: Thr40 is replaced with Ala37, Ser47 with Ala45, Tyr48 with Phe46, Asn52 with Leu50, and Tyr67 with Trp65. Cytochrome c_H is the only cytochrome *c*, which has a tryptophan (Trp65) in the position normally occupied by Tyr67, and the only one known to lack the internal water, or hydroxyl equivalent, and its associated hydrogen bonding network, in the left-hand side of the haem cleft.

Considerable speculation has centered around the role of tyrosine (tuna, Tyr67) in modulating redox potential. Only 2% of cytochromes *c* or c_2 have an alternative (phenylalanine) at this position (Moore & Pettigrew, 1990). No cytochrome has been investigated in which Tyr67 has been modified to a tryptophan, but a number of variants have been investigated in which it has been modified (chemically or by mutagenesis) to the relatively hydrophobic phenylalanine. If this had led to no changes except for a change in hydrophobicity then the mutation would be expected to lead to a higher redox potential as observed in cytochrome c_H; however, in all cases the redox potential was decreased by 30–60 mV (Luntz et al., 1989; Wallace et al., 1989; Caffrey et al., 1991; Berghuis et al., 1994). An explanation of this observation has been afforded by determination of the complete structures of oxidized and reduced forms of the wild-type (Tyr67) and the Tyr67Phe variant of the iso-1-cytochrome *c* of yeast by Berghuis et al. (1994). They have shown that the mutation does not lead to an overall increase in hydrophobicity because in this variant the usual water (Wat166) is retained and a second water is present in an enlarged internal cavity, in a position approximately equivalent to that of the hydroxyl group of Tyr67 in the wild-type protein. The mutation also leads to alterations in the hydrogen bond network seen in wild-type cytochrome *c*, involving Tyr67, Wat166 (tuna, Wat3), and other nearby residues, and loss of the Tyr67 to Met80 hydrogen bond normally present in the reduced form. It was concluded that these alterations lead to a structurally more rigid and stable form of the oxidized protein and hence a substantially lower midpoint potential in the variant (Berghuis & Brayer, 1992).

A further structural feature of cytochromes that has been implicated in the regulation of redox potential is the salt bridge between the inner haem propionate (HP7) and Arg38, replacement of which by other amino acids leads to a substantial decrease in redox potential (Proudfoot & Wallace, 1987). This is consistent with the suggestion of Moore et al. (1984) that the positive charge on the guanidino group of Arg38 effectively neutralizes the negatively charged inner propionate, thus diminishing its potential electro-

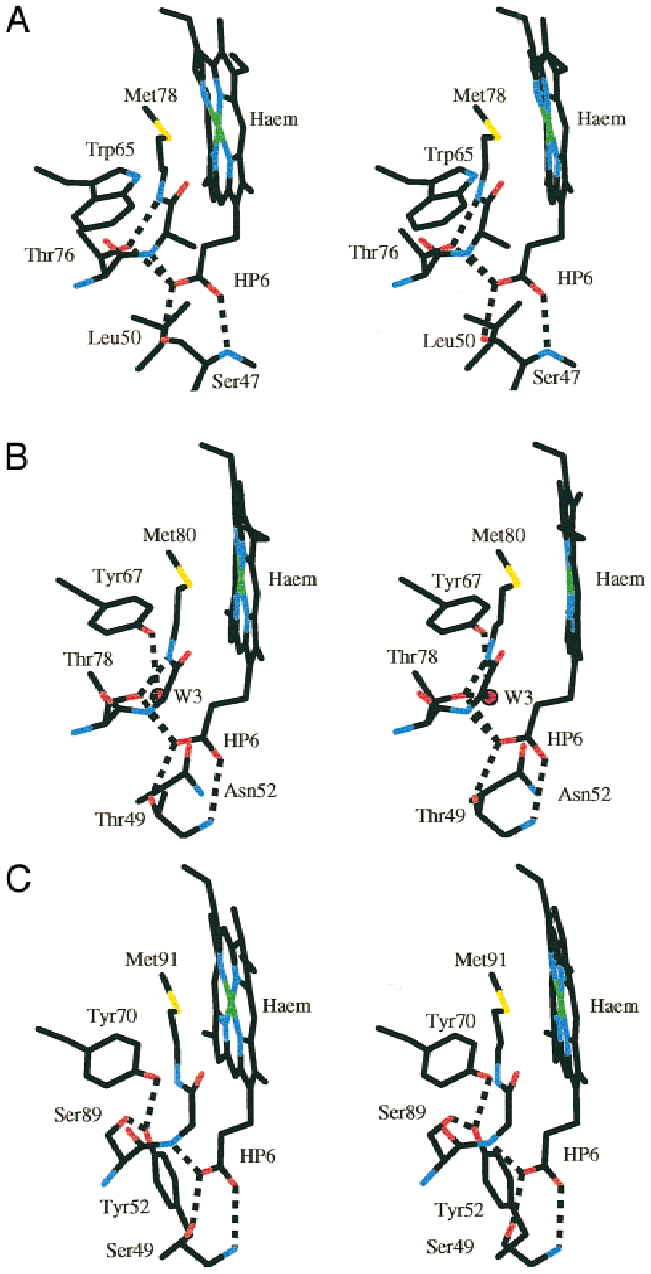

Fig. 4. Stereo diagrams of the left-hand channel of the haem binding site in the oxidized cytochromes. The inner propionate (HP7) is omitted for clarity. **A:** Cytochrome c_H; although the hydrogen bonding pattern of the outer propionate (HP6) is the same as in the other two cytochromes, Tyr67 is replaced by Trp65 and there is no buried water. **B:** Cytochrome *c* (tuna); Tyr67 is hydrogen bonded to the buried water (W3). Asn52 forms additional bonds with W3 and HP7 in the reduced cytochrome. **C:** Cytochrome c_2 from *R. rubrum*. Asn52 in tuna is replaced by a tyrosine whose side-chain hydroxyl group occupies the same position as the conserved water molecule. These diagrams were produced using MOLSCRIPT (Kraulis, 1991).

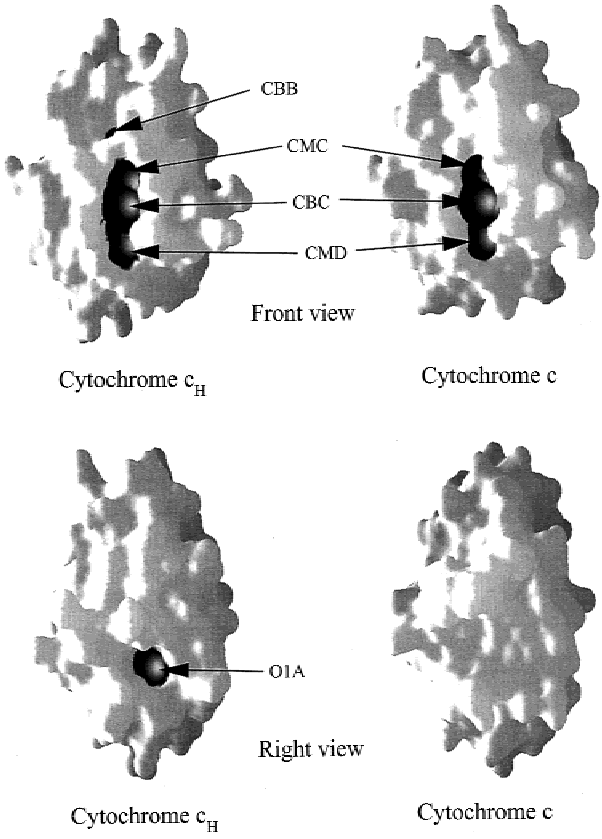

Fig. 5. The solvent exposed regions of haem in cytochrome c_H and tuna cytochrome *c*. The solvent exposed regions of the haem (in black) were calculated using a rolling ball of 1.4 Å radius in GRASP (Nicholls et al., 1993). Tuna cytochrome *c* has atoms CMC, CBC, and CMD of the haem exposed; in addition to these, cytochrome c_H also has atom CBB exposed on the front surface and atom OIA of the inner haem propionate (HP7) exposed on the lower right-hand side of the molecule.

static effect at the haem iron and thereby raising the observed midpoint potential. The propionate (HP7) of cytochrome c_H is unable to form such a salt bridge, because Arg38 is replaced by Ala35, which should lower the redox potential for cytochrome c_H. We suggest that the observed redox potential of cytochrome c_H is achieved by the delicate balance of these opposing influences, between hydrophobicity of the left side of the haem cleft on the one hand, and the absence of Arg38 and increased haem exposure on the other.

The relevance of the cytochrome c_H structure to the electron transfer mechanism

In cytochrome *c* the buried water (tuna, Wat3) is part of a hydrogen bonding network involving Thr78, and the outer haem propionate (HP6) (Fig. 4). In the reduced state, the water is also bonded to Asn52, and Tyr67 is hydrogen bonded to the sulfur of the Met80 ligand. During oxidation these two bonds are broken, with a corresponding shift in the side chains of Asn52 and Tyr67, and the water molecule is shifted about 1.2 Å toward the iron. This conformational change is likely to occur in response to, or alternatively to stabilize, the increased positive charge centered at the haem iron in the oxidized form (Louie & Brayer, 1990). It has been suggested that the consistency of these observations across all available cytochrome *c* structures strongly implicates this water and its hydrogen bonding network in their electron transfer mechanisms (Brayer & Murphy, 1996). However, in cytochrome c_H the

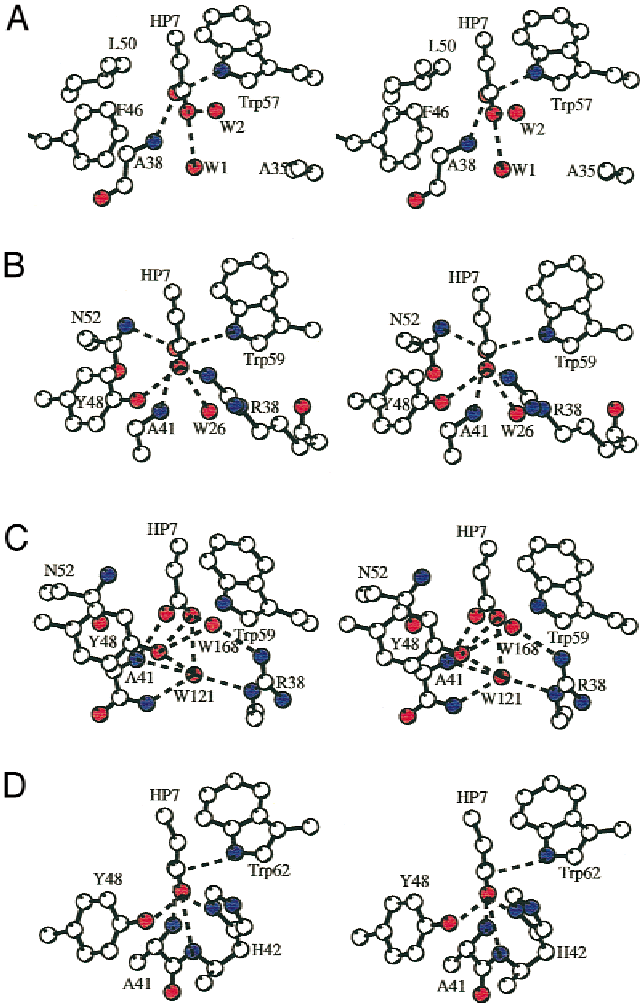

Fig. 6. Stereo diagrams of the hydrogen bonding patterns surrounding the inner haem propionate HP7. **A:** Cytochrome c_H; the highly conserved Arg38 (tuna) is replaced by Ala35 allowing access of the bulk solvent to the inner propionate HP-7, which is an otherwise relatively hydrophobic environment. **B:** Tuna cytochrome *c*, in which the inner propionate is shielded from the bulk solvent by Arg38. **C:** Yeast iso-1 cytochrome *c*; Arg38 is connected to the propionate via W121 (equivalent to tuna Wat26) and an additional water (W168) forming a rigid network, which shields the propionate from the bulk solvent; in this cytochrome Trp59 and Asn52 do not bond with the inner propionate. **D:** *R. rubrum* cytochrome c_2; the side chain of the highly conserved Arg38 is replaced by the side chain of His42, which forms an electrostatic link with the inner propionate, protecting it from the bulk solvent and preventing the usually conserved water (Wat26) from being present. These diagrams were produced using MOLSCRIPT (Kraulis, 1991).

unique structure of the left-hand side of its haem cleft, lacking water and the associated hydrogen bonding web, precludes such a mechanism. Thr76 (tuna, Thr78) is bonded to the outer haem propionate (HP6) as in other cytochromes, but Asn52 is replaced by Leu50, and the tryptophan (Trp65) is unable to form hydrogen bonds with the methionine ligand to the haem iron (Fig. 4).

Any structural changes that take place during oxidation and reduction of cytochrome c_H must do so in the unusually hydrophobic environment in its haem cleft, and these are likely to involve the novel Trp65, which replaces the conserved Tyr67. Trp65

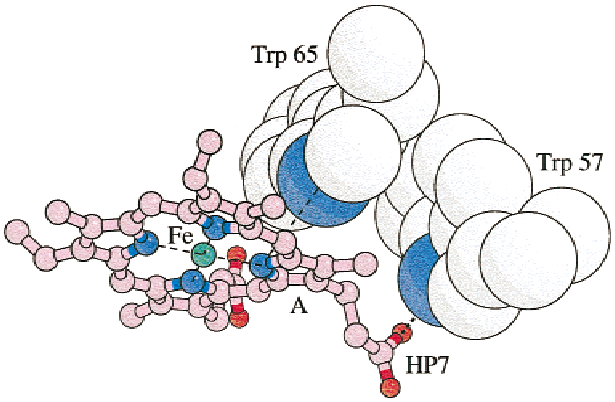

Fig. 7. The packing of Trp57 and Trp65 adjacent to the haem in cytochrome c_H showing hydrogen bond interactions between the indole NE1 of Trp57 and the inner haem propionate HP7 and a potential hydrogen bond between Trp65 and the ring A haem π cloud.

is unlikely to form a hydrogen bond to the iron ligand (Met78) in the ferrocytochrome as this would require a large rotation of the tryptophan side chain, which could only occur if there were a major change in the overall structure in this region. It is much more probable that Trp65 is involved in an alternative mechanism. The ring plane of Trp65 is inclined by about 15° from an orthogonal disposition with respect to ring A of the haem such that the indole NH is directed toward the pyrrole nitrogen (3.5 Å distant) (Fig. 7). Small rotational or translational adjustments to the position of Trp65 would permit the closer approach of NE1 to the haem plane where the π cloud is able to fill the role of acceptor for a hydrogen bond. Such hydrogen bond systems were first discussed by Levitt and Perutz (1988), and a number of examples have subsequently been identified (Mitchell et al., 1994). In the current context, this would provide an effective means for modulating the relative stability of the reduced and oxidized states. Furthermore, Trp65 is in van der Waals contact with the Trp57 side chain that in turn hydrogen bonds to the HP7 propionate (Fig. 7), thus perhaps contributing to the remarkable pH dependence of redox potential.

Other changes that have been observed on reduction of mitochondrial cytochrome *c* include the conformation of the loops that interconnect the inside and outside of the protein in the region of the haem pocket cleft. On the basis of work with the yeast cytochrome *c*, a model has been proposed that links the changes in the hydrogen bonding network with changes in conformation of the more mobile surface loops (Berghuis & Brayer, 1992; Brayer & Murphy, 1996). It was suggested that the relatively rigid 73–80 segment, by virtue of its surface location next to the solvent exposed edge of the haem, can act to trigger the structural changes required to stabilize the oxidation state required to facilitate electron transfer. On forming a complex with redox partners, the 75–78 β turn residues act as a "push button," which leads to a change in conformation involving movement of three mobile loops (tuna 47–59; 65–72; 81–85). Although cytochrome c_H retains the relatively immobile region (Lys71–Met78), only two of the three mobile loops are retained; the third is the critical loop (Lys63–Pro70) that carries the conserved tyrosine in cytochromes *c* and c_2 (tuna, Tyr67), which is uniquely replaced by tryptophan (Trp65) in cytochrome c_H, leading to a generally more rigid structure in this region. Clearly, in cytochrome c_H, no such mechanism can be

involved during its oxidation and reduction, and it should be noted that such conformational changes are not, in principle, essential for these redox reactions. Indeed, this is indicated by the observation that in the Tyr67Phe variant of yeast iso-1-cytochrome *c* system there is relatively little difference in the conformations of the oxidized and reduced forms and yet it is able to fulfill its functions almost as well as the wild-type protein (Berghuis et al., 1994).

Finally, we should consider whether or not there is any reason for cytochrome c_H to have the very special structure that it does. A possible explanation is that this has evolved to provide a relatively high redox potential, which may be essential for its additional special function in the "methanol oxidase" electron transport chain (Anthony, 1992). It is similar to other cytochromes *c* in mediating electron transfer between the cytochrome bc_1 complex and the oxidase, but it has the special additional function of oxidizing the cytochrome c_L that is the specific electron acceptor from methanol dehydrogenase. This cytochrome has a typical redox potential (254 mV) (O'Keeffe & Anthony, 1980) and a cytochrome *c* with a higher redox potential will facilitate its oxidation.

Materials and methods

Crystallization and data collection

The protein was purified as previously described (Day & Anthony, 1990). Initial crystallization conditions were found using the Hampton sparse matrix screen and optimized on the initial conditions found (screen 1 no. 43—30% PEG 1500, unbuffered). Crystals were grown using the hanging drop vapor diffusion method. The final conditions were 10 mg/mL protein, 18% PEG 1500, 50 mM Tris-HCl, pH 7.0. Crystals appeared within 2 days with dimensions of 200 μm × 200 μm × 100 μm. X-ray data were collected on a Mar 30 cm Image plate at room temperature. The X-ray source was an Enraf Nonius rotating anode generator operated at 50 kV and 100 mA producing copper Kα radiation via a graphite monochromator. The crystal to detector distance was 150 mm giving a maximum resolution of 2 Å at the edge of the plate. Data processing statistics are given in Table 2. The space group is P1, with the following cell dimensions: $a = 33.76$ Å, $b = 57.57$ Å, $c = 50.95$ Å, $\alpha = 67.81°$, $\beta = 89.33°$, and $\gamma = 74.40°$. Assuming three molecules per triclinic unit cell, a solvent content of 40% was calculated for the crystal.

Table 2. *Data processing and refinement statistics for the cytochrome c_H structure*

	Total	Highest resolution shell (2.07–2.01 Å)
Data processing		
R_{merge} [a]	6.1%	13.4%
χ^2 [b]	1.52	1.32
$\langle\sigma(I)\rangle$	740	265
$\langle I\rangle$	12,043	1,682
Redundancy	2.25	1.9
Completeness	94.4%	71.5%
Refinement statistics		
Resolution range (Å)	30–2.01	
Number of atoms	2,445 (2,160 protein, 129 haem, 156 waters)	
Number of parameters refined	9,951	
Number of reflections used	16,999	
R-factor [c] (%)	16.1	
Correlation coefficient (b)	0.96	
Free-*R* factor [d] (%)	22.2	
Correlation coefficient [e] (free set) (b)	0.92	
Average *B* main chain (Å^2)	25.2	
Average *B* protein atoms (Å^2)	30.5	
Average *B* waters (Å^2)	42.6	
Overall *B* (Å^2)	31.4	
RMSD from ideal geometry		
Bond lengths (Å)	0.007	
Bond angle distances (Å)	0.018	
Van der Waals contacts (Å)	0.028	
Type I planes (Å)	0.009	
Type II planes (Å)	0.007	
Chiral tetrahedra (Å)	0.011	

[a] $R_{merge} = \sum_h\sum_i|(I_{hi} - I_h)|/\sum_h\sum_i(I_{hi})$ where I_h is the mean of scaled observations I_{hi}.

[b] $\chi^2 = (\sum_h\sum_i[(I_{hi} - I_h)^2/\sigma^2(I_{hi})])\cdot n/(n - 1)$ where n = number of observations.

[c] Refinement *R*-factor $= \sum(|F_o| - |F_c|)/\sum F_o$ where F_o and F_c are the observed and calculated structure factors.

[d] The free *R*-factors were calculated with 5% of the reflection data.

[3] Correlation coefficient $= A/\sqrt{(BC)}$ where $A = n\sum(|F_o||F_c|) - (\sum|F_o|)(\sum|F_c|)$; $B = n\sum|F_o|^2 - (\sum|F_o|)^2$; $C = n\sum|F_c|^2 - (\sum|F_c|)^2$ and n = number of structure factors included. Fitting of structures was achieved using the LSQKB program, which uses the Kabsch algorithm (Kabsch, 1976).

Structure determination and refinement

The initial coordinate model used in molecular replacement was for cytochrome c_2 from *R. rubrum*, having removed those regions where the sequence alignment indicated major insertions relative to cytochrome c_H. The orientations of the three molecules in the cytochrome c_H unit cell were determined from a cross-rotation function calculated with ALMN where the solutions were the three highest peaks. An oriented search molecule was positioned at the origin of the P1 cell for cytochrome c_H. The translation vector for each of the other two molecules was calculated using TFFC. The peak height for the second and third molecule translations was 9.25 (map RMS 4.26) and 10.85 (RMS 4.74). Having applied appropriate rotations and translations to the *R. rubrum* cytochrome c_2 coordinates, the model was subjected to rigid body and subsequent restrained positional, and thermal parameter, refinement with RESTRAIN (Haneef et al., 1985). Five percent of data was flagged for the Free-*R* set. The first electron density maps were averaged using density modification. Unless otherwise stated, all calculations were performed using programs in the CCP4 suite (CCP4, 1994). Modeling was carried out using the X-Autofit-Autobuild option of QUANTA (Molecular Simulations, Inc., Burlington, Massachusetts). The initial difference and double difference maps showed clearly the location of sequence differences from the search model and regions where main-chain adjustments were required. Although good electron density was found for most regions, the loops 38 to 42 and 46 to 55 were less clearly defined. It was possible to trace the loop from residues 46 to 55 using the superposed coordinates for oxidized horse heart cytochrome *c*. The sequence of residues 38 to 42 fitted the electron density poorly and so this region was resequenced. The new sequence fitted the electron density much

better, although this region still displayed high thermal parameters. After fitting of the main-chain atoms and further positional refinement, NCS restraints were removed and waters added.

The structure of cytochrome c_H was refined to an *R*-factor of 16.5% with a corresponding R_{free} of 22.2%; the data processing and refinement statistics are given in Table 2. The RMSDs of main-chain and side-chain atoms between the three molecules of cytochrome c_H in the unit cell were 0.29–0.34 and 0.66–0.78 Å, respectively. Fitting of structures was achieved using the LSQKB program, which uses the Kabsch algorithm (Kabsch, 1976).

Acknowledgments

We acknowledge financial support from BBSRC and The Wellcome Trust.

References

Anthony C. 1992. The c-type cytochromes of methylotrophic bacteria. *Biochim Biophys Acta 1099*:1–15.

Anthony C, Ghosh M. 1998. The structure and function of the PQQ-containing quinoprotein dehydrogenases. *Prog Biophys Mol Biol 69*:1–21.

Baistrocchi P, Banci L, Bertini I, Turano P. 1996. Three-dimensional solution structure of *Saccharomyces cerevisae* reduced Iso-1-cytochrome *c*. *Biochemistry 35*:13788–13796.

Banci L, Bertini I, Bren KL, Gray HB, Sompornpisut P, Turano P. 1997a. Solution structure of oxidized *Saccharomyces cerevisae* Iso-1-cytochrome *c*. *Biochemistry 36*:8992–9001.

Banci L, Bertini I, Gray HB, Luchinat C, Reddig T, Rosato A, Turano P. 1997b. Solution structure of oxidized horse heart cytochrome c_2. *Biochemistry 36*:9867–9877.

Benning MM, Meyer TE, Holden HM. 1996. Molecular structure of a high potential cytochrome c_2 from *Rhodopila globiformis*. *Arch Biochem Biophys 333*:338–348.

Berghuis AM, Brayer GD. 1992. Oxidation state conformational changes in cytochrome *c*. *J Mol Biol 223*:259–276.

Berghuis AM, Guillemette JG, Smith M, Brayer GD. 1994. Mutation of tyrosine-67 to phenylalanine in cytochrome *c* significantly alters the local heme environment. *J Mol Biol 235*:1326–1341.

Brayer GD, Murphy MP. 1996. Structural studies of eukaryotic cytochromes *c*. In: Scott RA, Mauk AG, eds. *Cytochrome c. A multidisciplinary approach*. Sausalito, California: University Science Books.

Bushnell GW, Louie GV, Brayer GB. 1990. High resolution structure of horse heart cytochrome *c*. *J Mol Biol 214*:585–595.

Caffrey MS, Daldal F, Holden HM, Cusanovitch MA. 1991. Importance of hydrogen-bonding networks in cytochromes *c* to their redox potentials and stabilities. *Biochemistry 30*:4119–4125.

Collaborative Computational Project, No. 4. 1994. The CCP4 suite: Programmes for protein crystallography. *Acta Cryst D50*:760–763.

Cox JM, Day DJ, Anthony C. 1992. The interaction of methanol dehydrogenase and its electron acceptor, cytochrome c_L, in the facultative methylotroph *Methylobacterium extorquens* AM1 and in the obligate methylotroph *Methylophilus methylotrophus*. *Biochim Biophys Acta 1119*:97–106.

Day DJ, Anthony C. 1990. Soluble cytochromes *c* of methanol-utilising bacteria. *Methods Enzymol 188*:298–303.

Ghosh M, Anthony C, Harlos K, Goodwin MG, Blake CCF. 1995. The refined structure of the quinoprotein methanol dehydrogenase from *Methylobacterium extorquens* at 1.94Å. *Structure 3*:177–187.

Haneef I, Moss DS, Stanford MJ, Borkakoti N. 1985. Restrained structure factor least-squares refinement of protein structures using a vector processing computer. *Acta Cryst A41*:426–423.

Kabsch W. 1976. A solution for the best rotation to relate two sets of vectors. *Acta Cryst A32*:922–923.

Kassner RJ. 1972. Effects of nonpolar environments on the edox potentials of heme complexes. *Proc Nat Acad Sci USA 69*:2263–2267.

Kraulis PJ. 1991. MOLSCRIPT: A program to produce both detailed and schematic plots of protein structures. *J Appl Cryst 24*:946–950.

Laskowski RA, MacArthur MW, Moss DS, Thornton JM. 1993. PROCHECK: A program to check the quality of protein structures. *J Appl Cryst 24*:946–950.

Levitt M, Perutz M. 1988. Aromatic rings as hydrogen bond acceptors. *J Mol Biol 201*:751–754.

Louie GV, Brayer GB. 1990. High resolution refinement of yeast-iso-1-cytochrome *c* and comparison with other eucaryotic cytochromes *c*. *J Mol Biol 214*:527–555.

Luntz TL, Schejter A, Garber EAE, Margoliash E. 1989. Structural significance of an internal water molecule studied by site-directed mutagenesis of tyrosine-67 in rat cytochrome *c*. *Proc Nat Acad Sci USA 86*:3524–3528.

Mitchell JBO, Nandi CL, McDonald IK, Thornton JM, Price SL. 1994. Amino/aromatic interactions in proteins: Is the evidence stacked against hydrogen bonding. *J Mol Biol 239*:315–331.

Moore GR, Harris DE, Leitch FA, Pettigrew GW. 1984. Characterisation of ionisations that influence the redox potential of mitochondrial cytochrome *c* and photosynthetic bacterial cytochrome c_2. *Biochim Biophys Acta 754*:331–342.

Moore GR, Pettigrew GW. 1990. *Cytochromes c; evolutionary, structural and physicochemical aspects*. London: Academic Press. pp 1–478.

Nicholls A, Bharadwaj R, Honig B. 1993. GRASP: A graphical representation and analysis of surface properties. *Biophys J 64*:A166.

O'Keeffe DT, Anthony C. 1980. The two cytochromes c in the facultative methylotroph *Pseudomonas* AM1. *Biochem J 192*:411–419.

Proudfoot AEI, Wallace CJA. 1987. Semisynthesis of cytochrome *c* analogs. The effect of modifying the conserved residue 38 and residue 39. *Biochem J 248*:965–967.

Qi PX, Distefano DL, Wand AJ. 1994. Solution structure of horse heart ferrocytochrome *c* determined by high-resolution NMR and restrained simulated annealing. *Biochemistry 33*:6408–6417.

Salemme FR, Freer ST, Xuong NH, Alden RA, Kraut J. 1973. The structure of oxidized cytochrome c_2 of *Rhodospirillum rubrum*. *J Biol Chem 248*:3910–3921.

Scott RA, Mauk AG. 1996. Cytochrome *c*. A multidisciplinary approach. Sausalito, California: University Science Books.

Surridge C. 1994. Watershed for the structure of cytochrome *c*. *Nature 369*:426.

Tanako T, Dickerson RE. 1981a. Conformation change of cytochrome *c*. I. Ferrocytochrome *c* structure refined at 1.5 Å resolution. *J Mol Biol 153*:79–94.

Tanako T, Dickerson RE. 1981b. Conformation change of cytochrome *c*. II. Ferricytochrome *c* structure refinement at 1.8 Å resolution and comparison with the ferrocytochrome structure. *J Mol Biol 153*:95–115.

Wallace CJA, Mascagni P, Chait BT, Collawn JF, Paterson Y, Proudfoot AEI, Kent SBH. 1989. Substitutions engineered by chemical synthesis at 3 conserved sites in mitochondrial cytochrome *c*—Thermodynamic and functional consequences. *J Biol Chem 264*:15199–15209.